# Potential of satellite imagery to detect seagrass (Zostera) patches in Hawke's Bay

*Prepared for Hawke's Bay Regional Council*

*June 2020*

Prepared by:
Alexandre C. G. Schimel

For any information regarding this report please contact:
Alexandre C. G. Schimel

Fisheries Acoustics & Monitoring
+64-4-386 0510
alexandre.schimel@niwa.co.nz

National Institute of Water & Atmospheric Research Ltd
Private Bag 14901
Kilbirnie
Wellington 6241

Phone +64 4 386 0300

NIWA CLIENT REPORT No: 2020188WN
Report date: June 2020
NIWA Project: ELF20305

| Quality Assurance Statement | | |
|---|---|---|
|  | Reviewed by: | Neale Hudson |
|  | Formatting checked by: | Alex Quigley |
|  | Approved for release by: | Steve Wilcox |

# Contents



## Tables



## Figures

# Executive summary

Seagrasses are marine plants that provide many important ecosystem services and contribute to nutrient cycling and marine carbon sequestration, but that have been declining at an accelerating rate globally. In New Zealand, the indigenous seagrass *Zostera muelleri* has also been declining over the past decades. In the Hawke's Bay region, *Zostera* occurs as isolated patches, and historic and present-day coverage extent is unknown. Since the effective management and conservation of seagrass requires identifying its current extent and monitoring change in this extent over time, the Hawke's Bay Regional Council (HBRC) is considering using remote sensing methods to visualise the entire coast and assess seagrass coverage consistently throughout the region.

At regional spatial scales, a common alternative to aerial photography is satellite imagery. However, seagrass in Hawke's Bay can occur as small (~2-3 m), relatively widely scattered patches. It is uncertain whether remnant patches of these dimensions can be detected with satellite imagery, which typically has a much coarser resolution than aerial photography. As a result, HBRC commissioned a review to better understand the potential of satellite imagery technology for mapping seagrass in the Hawke's Bay region.

In this review, we identify several relevant institutional and commercial satellite imagery providers and investigate the use of their product for seagrass mapping in the recent scientific literature. We discuss the critical factors that influence our ability to use these products for mapping the location of remnant seagrass patches, including spatial resolution, spectral resolution, and the effects of water depth.

We conclude that the detection and mapping of seagrass with multispectral satellite imagery is a mature field, that automated classification methods are able to detect seagrass beds accurately, but that it is uncertain whether the scarce seagrass patches in Hawke's Bay can be detected using these products, primarily due to the low dimensions of the patches relative to the spatial resolution of the imagery available. Only an experiment with suitable sample imagery over a known area would allow us to conclude whether an effective automated detection method can be devised and subsequently applied at larger scale. We identified the most suitable imagery source (finest spatial and spectral resolution) as WorldView-2 and WorldView-3 by Maxar Technologies, and provide indicative pricing and contact information.

We also recommend investigating airborne hyperspectral imagery as an alternative source of remote sensing imagery due to its finer spatial and spectral resolution. Finally, we also advise that the relevant scientific literature is reviewed periodically as remote sensing platforms, sensors, and imagery processing methods are currently experiencing a strong phase of technological development, which may alter the conclusions of this assessment in the very near future.

# 1 Introduction

Seagrasses are flowering plants growing in marine environments, typically shallow sub-tidal and inter-tidal soft sediments beds or veneers. Over 60 seagrass species belonging to four different families exist across the world (Green and Short 2003). Seagrasses provide many important ecosystem services, including the primary production that supports a high diversity of associated fauna, creating habitat for invertebrate and juvenile fish species, providing coastal stabilisation, and promoting the settlement of fine sediments (Hemminga and Duarte 2000). It has been estimated that they contribute the equivalent of (USD) $1.9 trillion in nutrient cycling globally (Waycott et al. 2009) and sequester between 10 and 20% of global oceanic carbon annually despite occupying less than 0.2% of the area of the world's oceans (Fourqurean et al. 2012). Despite this recognized importance, seagrass coverage around the world has been declining at an accelerating rate due to anthropogenic and natural disturbances (Waycott et al. 2009; Arias-Ortiz et al. 2018). New Zealand has one species of seagrass, the indigenous *Zostera muelleri*, which is found primarily intertidally across the country (Turner and Schwarz 2006). The limited information available suggests that *Zostera* has experienced a major decline in New Zealand over the past decades, especially when growing subtidally (Inglis 2003; Turner and Schwarz 2006; Matheson et al. 2011). For example, in Tauranga Harbour (Bay of Plenty), more than 14,000 ha of seagrass have been lost since 1959, with 90% loss of subtidal beds (Park 1999; 2016). In contrast, natural recolonization has been recently documented in some regional locations, including the Waitematā Harbour and the Whangārei Harbour (Lundquist et al. 2018).

Around Hawke's Bay, *Zostera* is sparsely found today, and both past and present coverage extent is mostly unknown (Matheson 2018), but a range of coverage dynamics has been documented: once present in the Ahuriri estuary, it is now entirely lost (Haggit and Wade 2016); remnant patches have been recently found in the Pōrangahau estuary (Matheson 2018); and recent and rapid recolonization has been observed at an intertidal reef in Kairākau (Madarasz-Smith and Shanahan 2020).

Effective management and conservation of seagrass requires (among other things) a better knowledge and understanding of these various dynamics. Mapping the historical and current extent of seagrass and monitoring future change in this extent would allow specific areas to be targeted and prioritized for management and/or restoration. This mapping objective may be applied at a range of scales, determined by the extent of the management area: local (i.e., a single estuary), regional, national, or global. *In-situ* techniques for assessing the condition of seagrass, such as field or diver-based surveys, do not scale up effectively beyond the local level, which makes monitoring of seagrass extent at larger scales only realistically achievable using remote sensing technology (Hedley et al. 2016). The earliest and currently most widely used remote sensing approach is visual interpretation of aerial photographs (Uhrin and Townsend 2016); it is relatively simple, which makes it suitable as a standard technique for management purposes (Robertson et al. 2002). However, there have been many technological developments in remote sensing over the past decades, both in platforms (satellites and drones) and in sensors. These are often tested for seagrass mapping after they arise and many have been adopted when affordable and relevant (Hossain et al. 2014; Pham et al. 2019).

Hawke's Bay Regional Council (HBRC) used aerial photography to assess the current and historical presence of seagrass in one of its estuaries (Matheson 2018). They also trialled the use of drone imagery. They are now considering remote sensing methods that could make it possible to visualise the entire coast. If successful, these methods would make it possible to assess seagrass coverage in a

consistent manner throughout the region. Satellite imagery could be an alternative to aerial photography for regional scale survey, but seagrass in Hawke's Bay can occur as small (~2-3 $m^2$), scattered patches so it is uncertain whether these could be detected with satellite imagery, which typically has a much coarser resolution than aerial photography. As a result, HBRC has engaged NIWA to review the potential of satellite imagery technology for mapping seagrass in the Hawke's Bay region.

In this short report, we provide a review of the relevant scientific literature, satellite imagery data service providers (institutional and commercial), and mapping methods, with a focus on the foreseeable limitations of this approach to the case of the fragmented distribution of seagrass in Hawke's Bay. This assessment will assist HBRC to assess the potential of this technology for large-scale and long-term monitoring of seagrass in Hawke's Bay. This report was funded through an MBIE Envirolink Small Advice Grant (HBRC256, MBIE Contract C01X1937).

# 2 Background

## 2.1 Remote sensing

Remote sensing is the process of detecting and monitoring the physical characteristics of an object or area by measuring its reflected or emitted radiation at a distance. Whilst this description applies to many technologies (e.g., medical imagery), it is mostly commonly used in reference to sensors carried by airborne (e.g., planes, drone) or spaceborne (i.e., satellites) sensors, which measure radiation in a portion of the electromagnetic spectrum (e.g., visible light, infrared, radio waves, etc.) that was reflected or radiated from objects on the surface of the Earth.

Digital aerial photography - the most readily understandable remote sensing technology – consists of recording light within three bands in the Red, Green, and Blue (RGB) sections of the visible spectrum, and combining them on an RGB display to produce an immediately familiar "true-colour" image of the surface of the earth. Since this imagery is familiar, the land type of interest (e.g., seagrass) can be identified and its extent digitized manually. In effect, the operator recognizes on the imagery instances of the land type of interest based on its representative spectral (colour), textural (spatial variations in colour), spatial (size, extent, shape), and contextual (surroundings) properties.

Multispectral sensors are remote sensing instruments that acquire data from more than just three bands in the visible spectrum (Figure 1). The most common additional bands are in the near-infrared region of the electromagnetic spectrum, because of relevance to identify healthy vegetation (chlorophyll strongly absorbs blue and red light but strongly reflects infrared light). More complex multispectral sensors installed on scientific satellites may acquire data in other regions of the infrared (e.g., short-wave infrared, thermal infrared), or in different regions of the visible spectrum (e.g., "coastal/aerosol" is the common name for a band in the deep blue). Since different types of land and objects on the surface tend to present different reflection spectra, the major interest in a sensor that provides increased spectral richness (such as a multispectral sensor *versus* RGB sensors) is an increased ability to interpret objects occurring within an image using their spectral and textural properties. The trade-off of this richness is that the information embedded within this data type is not as immediately recognizable as that in an RGB photograph, which calls for more automated interpretation approaches.

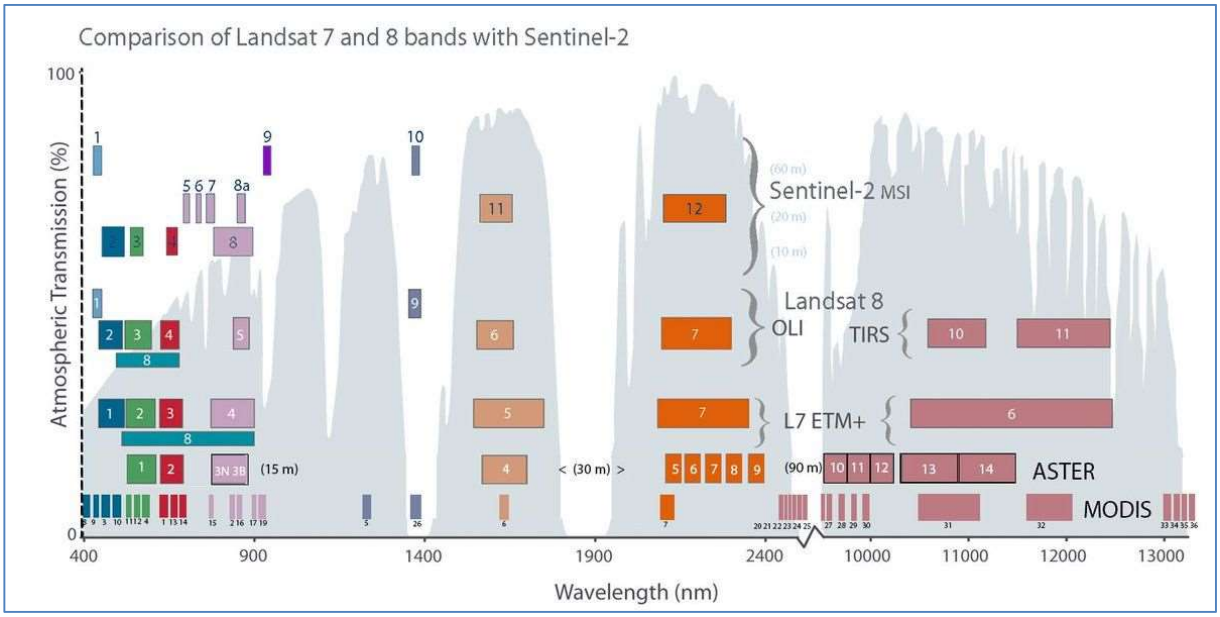


**Figure 1: Bands sampled by some frequently used satellite multispectral sensors superimposed on the spectrum of atmospheric transmission.** Information shown is for MSI on Sentinel-2, OLI and TIRS on Landsat 8, ETM+ on Landsat 7, ASTER on Terra, and MODIS on Aqua and Terra. From left to right, the bands coloured in blue, green and red are in the visible spectrum; the bands coloured in purple are in the near infrared; the bands coloured in light and dark orange are in the Short-Wave Infrared (SWIR); and the bands coloured in mauve are in the Thermal Infrared (TIR). Figure from https://landsat.gsfc.nasa.gov/.

Hyperspectral sensors extend the concept of using increased spectral richness to increase image interpretation capability. While multispectral sensors record reflected radiation within up to a dozen, non-necessarily adjacent, wide bands (over 15 nm, as illustrated in Figure 1), hyperspectral instruments record reflected radiation within hundreds of narrow and adjacent bands (≤~10 nm), covering the entire spectrum of interest (visible and/or infrared). This very high spectral resolution readily allows the identification of objects (vegetation species, mineral type, etc.) by comparing the acquired spectral data to libraries of known spectral signatures (Kutser et al. 2020).

RGB, multispectral, and hyperspectral sensors capture solar radiation reflected by objects on the earth's surface. Other types of remote sensing technologies generate and transmit the very radiation whose reflection they capture. These so-called "active" sensors include lidar and radar, which operate with visible light and radio waves, respectively.

Sensors based on these remote sensing technologies come in various size and weight, which may allow or restrict their deployment on some platforms. Particularly, drones have been mostly carrying RGB cameras until recently because more complex sensors were too heavy. Technological development in the past decade has produced lightweight versions of multispectral (usually, simple RGB cameras with one additional band in the infrared), hyperspectral, and lidar sensors, which can be deployed from some (powerful) drones. However, their use is not widespread yet because of the high cost of these modern sensors and the drones that can carry them.

## 2.2 Non-satellite remote sensing for seagrass mapping

Many combinations of platforms (drone, plane, satellites) and sensors (RGB, multispectral, hyperspectral, lidar, radar) have been trialled for their capability to map seagrass. As discussed previously, the manual interpretation of RGB airborne imagery is the earliest and most widely used remote sensing method to map seagrass at local and regional scales (Uhrin and Townsend 2016; Moniruzzaman et al. 2019). Drone surveys are increasingly used as they achieve higher resolution but over smaller spatial scales (Duffy et al. 2018). In the domain of research, airborne lidar have been trialled (Wang and Philpot 2007), while the use of airborne hyperspectral sensors has been explored in depth (e.g., Mumby et al. 1997; Phinn et al. 2008; Vahtmäe et al. 2012; Valle et al. 2015). This report focuses on the use of multispectral (and to a lesser extent, hyperspectral) satellite data for mapping seagrass. For more information on drone-based and airborne methods, recent general reviews on the topic of remote sensing for seagrass or other benthic types in acoustically shallow waters would be instructive, such as Hossain et al. (2014), Hedley et al. (2016), Moriuzzaman et al. (2019), Pham et al. (2019), or Kutser et al. (2020).

# 3 A review of satellite imagery for seagrass mapping

## 3.1 Scientific multispectral imagers

National space agencies (mainly NASA, ESA, JAXA) have been deploying and operating satellites with multispectral sensors for scientific research for several decades. Most of these systems have a spatial resolution that is too coarse for the purpose of mapping seagrass. Although some have been used for this purpose, such as the 250 m resolution imagery of the MODIS instrument aboard satellites Terra and Aqua (e.g., Petus et al. 2014), the resolution of the sensors are too coarse for the purpose of mapping small seagrass patches and are thus not considered further.

The earliest, and arguably still most commonly used, high-resolution satellite imaging technology used to map land cover types is from NASA's Landsat programme. The programme consists of a series of satellite missions initiated in 1972 with Landsat 1, followed by successor satellites for continuity in acquisition, and currently operating with Landsat 7 and 8 actively acquiring imagery. As imaging technology evolved over time, the mission series has made use of four types of multispectral sensors: Landsat MSS (on Landsat 1, 2, 3, 4, and 5), Landsat TM (on Landsat 4 and 5), Landsat ETM+ (on Landsat 7) and Landsat OLI (on Landsat 8). All these systems have been used to map seagrass at regional to national scales (e.g., Ackleson and Klemas 1987; Luczkovich et al. 1993; Mumby et al. 1997; Shapiro and Rohmann 2006; Phinn et al. 2008; Knudby et al. 2010; Lyons et al. 2012; Lyons et al. 2013; Kovacs et al. 2018).

In 2014, the European Space Agency (ESA) initiated the Copernicus programme, which consists of a series of satellite missions for a variety of scientific and commercial applications. The Sentinel-2 satellite was launched in 2017 as part of this programme, carrying the multispectral sensor MSI destined for land and coast imagery. Sentinel-2 MSI imagery has since been used for seagrass mapping at regional and national scales (Kovacs et al. 2018; Traganos et al. 2018; Traganos and Reinartz 2018; Bayyana et al. 2020).

The spatial resolution of Landsat 8 OLI data ranges from 15 m (band 8 – panchromatic) to 30 m (all other bands). The spatial resolution of Sentinel-2 MSI data starts at 10 m (bands 2, 3, 4 – visible, and band 2 – near-infrared). Current and archived imagery of the Landsat missions and the ESA Copernicus satellite missions, including Sentinel-2, may be accessed from a variety of sources, and imagery downloaded at no cost.

## 3.2 Commercial multispectral imagers

Commercial satellite imagery has been available for several decades, usually at a higher spatial resolution but lower spectral richness than the scientific satellite imagery available at the same time. Most of those commercial data typically consist of a panchromatic band and 4 individual bands in the visible and the near-infrared. The panchromatic band covers the entire visible spectrum, and is thus wider than all other bands, which implies a higher signal-to-noise ratio, and which translates into higher spatial resolution. A processing method called pansharpening is typically applied to combine the band data to obtain RGB imagery at the resolution of the panchromatic band. In the text that follows, spatial resolutions are written as X/Y with X being the best (nadir) resolution of the panchromatic band (and the pansharpened RBG imagery) and Y being the best resolution of the other visible and NIR bands. X and Y have units of length (m).

Data from most commercial imaging satellites have been used for mapping seagrass. These include:

- the 10/20 m resolution imagery from the earlier SPOT satellites (Israel and Fyfe 1996; Mumby et al. 1997),
- the 0.60/2.40 m resolution imagery of the QuickBird 2 satellite (Mishra et al. 2006; Phinn et al. 2008; Urbański et al. 2009; Lyons et al. 2011; Roelfsema et al. 2014), and
- the 0.82/3.28 m resolution from the IKONOS satellite (Mumby and Edwards 2002; Fornes et al. 2006; Knudby and Nordlund 2011; Roelfsema et al. 2014; Pu and Bell 2017).

Although these systems are now decommissioned, imagery archives are still available for purchase from their operators.

Most of the more recent systems, which are still actively acquiring imagery, have also been used to map seagrass, including:

- the 1.5/3 m imagery of the daily-imaging PlanetScope constellation (Asner et al. 2017),
- the 0.46/1.84 m imagery of the WorldView-2 satellite (Cerdeira-Estrada et al. 2012; Roelfsema et al. 2014; Manuputty et al. 2015; Marcello et al. 2015; Baumstark et al. 2016; Su and Huang 2019), and
- the 0.31/1.24 m imagery of WorldView-3 (Kovacs et al. 2018).

Overall, WorldView-2 and WorldView-3 are probably the most promising satellite imaging systems to date, not only because they provide the highest resolution available on the market at present, but also an unusually high spectral richness for commercial systems, with a total of 8 bands in the visible and near-infrared part of the spectrum (Figure 2).

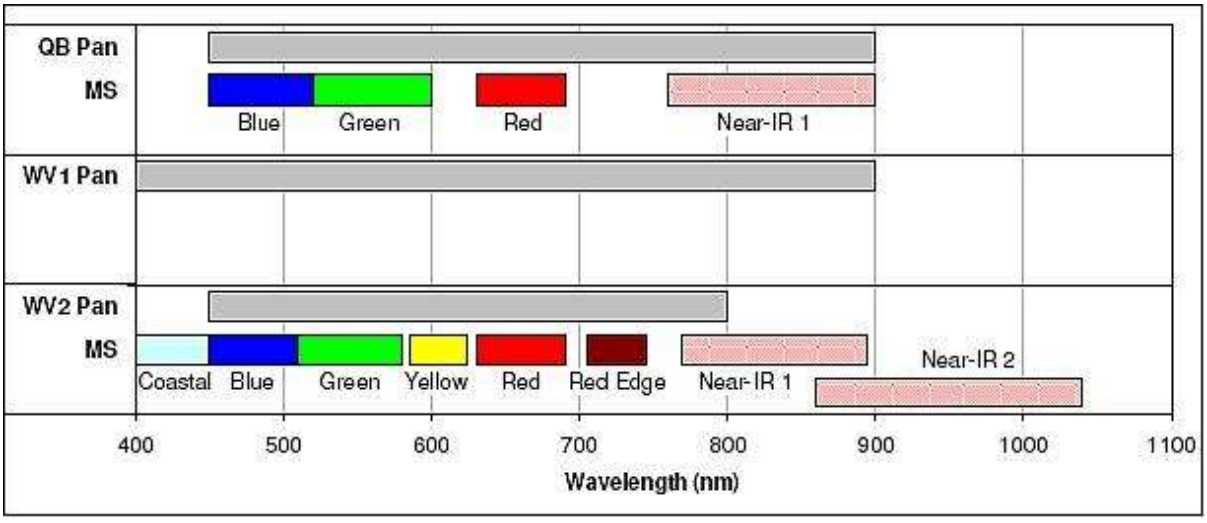


**Figure 2: Bands sampled by QuickBird 2, WorldView-1, and WorldView-2,3 instruments.** (image credit: Maxar/DigitalGlobe).

## 3.3 Hyperspectral imagers

Although less developed and less widely used than the airborne counterpart, spaceborne hyperspectral imaging is a readily available technology producing spectrally rich data at relatively high spatial resolutions. These include:

- CHRIS on satellite PROBA-1 (18-36 m resolution, launched 2001, active),
- Hyperion on satellite Earth Observation-1 (30 m resolution, launched 2001, decommissioned 2015),
- HICO on the International Space Station (90 m resolution, launched 2009, decommissioned 2014), and
- PRISMA on the satellite of the same name (30 m resolution, launched 2019, active).

Data from these sources are less commonly used than their multispectral counterparts, which is perhaps due to the increased complexity and volume of hyperspectral data. Some of these systems have been used to map seagrass, including CHRIS (Casal et al. 2011), Hyperion (Pu et al. 2012; Pu and Bell 2013), and HICO (Cho et al. 2014). More information on both airborne and spaceborne hyperspectral sensors for mapping seabed types in acoustically shallow waters, including seagrass, can be found in Kutser et al. (2020).

# 4 Discussion

## 4.1 Spatial resolution

Spatial resolution is normally defined as the minimum distance between two targets that allow a correct identification of two separate targets. Under this definition, spatial resolution only informs the *separability* between targets. However, spatial resolution is commonly understood as *ground sample distance*, which is the horizontal distance between two measurements, and specifically in digital products with *pixel size*, which is the distance between two image pixels. Under this definition, spatial resolution informs the more critical requirement regarding the *detectability* of the underlying target.

When visually interpreting RGB imagery, the size of an object usually needs to be at least 5 to 10 times the image pixel size to allow its detection. It is only from this size that sufficient context, colour, textural, and geometric information starts to become available for humans to positively identify an object. Textural analysis, or modern Object-Based Image Analysis (OBIA) methods of image classification resemble this human approach to processing an image using multidimensional information, and also require high spatial resolution in relation to the size of the objects to be detected. The minimum size of an identifiable object compared to the spatial resolution will often also be dependent on other issues that combine to affect the quality and usefulness of the imagery; these include imagery artefacts and inadequate correction for atmospheric effects and, for benthic types underwater such as some seagrass, light effects on the water surface (sunglint and sun glitter) and the absorption of light by water (see section on effects of water depth).

## 4.2 Spectral resolution

To some extent, a sensor's spectral richness may compensate for poor spatial resolution. If the land type of interest has a significantly different reflectance compared to its background in a captured frequency band – this may provide sufficient information to allow positive identification. Figure 3 shows an example of spectral signatures of sand and seagrass measured by Torres-Madronero et al. (2014). Above water, seagrass shows dramatically less reflectance than sand in the entire visible spectrum (from the ultraviolet/blue edge (400 nm) to the red edge (700 nm)). At 1 m water depth, seagrass has distinctive peaks in the green (~560 nm) and at the red edge (700 nm), compared to sand. In deeper waters, seagrass has a distinctive higher reflectance at the ultraviolet/blue edge (400 nm) compared to sand.

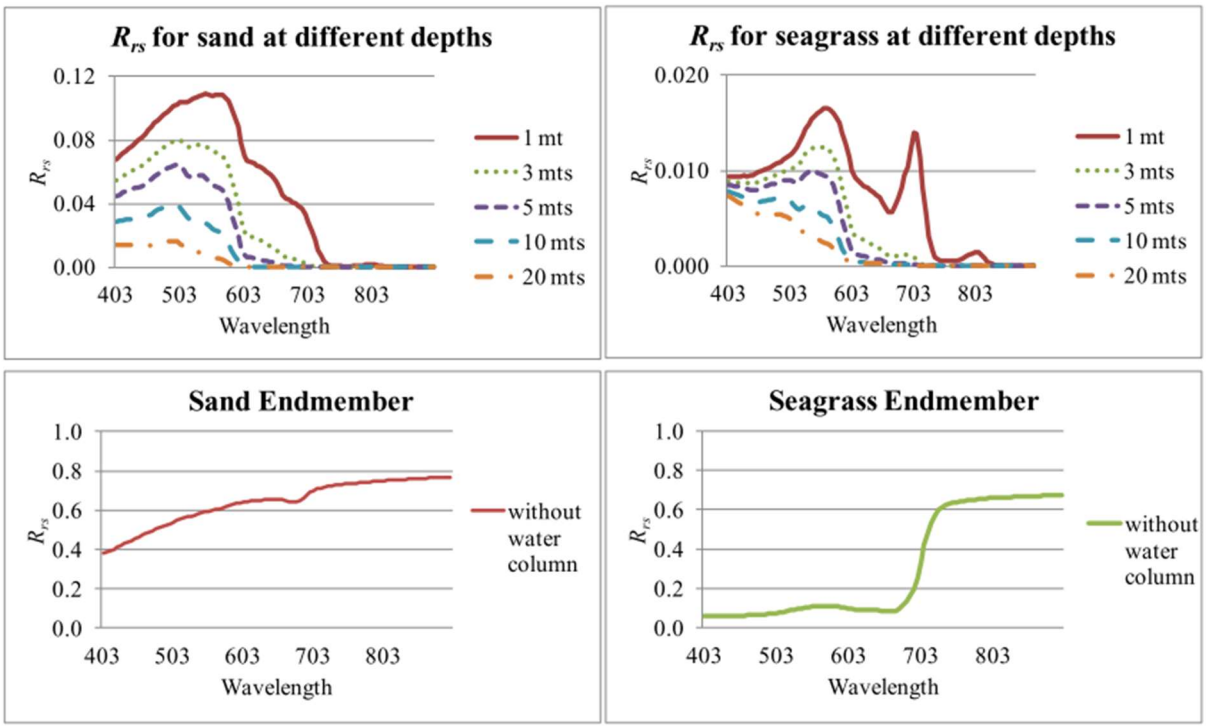


**Figure 3: Spectral signatures of sand and seagrass when not submerged, and at various depths.** Reproduced from Torres-Madronero et al. (2014) with permission.

These differences may be measurable in spectrally rich data and allow identification at spatial resolutions coarser than RGB imagery. Given enough spectral information, it is theoretically possible to detect seagrass even if its spatial extent is less than the imagery pixel size. Assuming that the value of a single pixel is only a function of the ground type(s) it covers, a pixel covering mixed types would have a value that reflects this mixed origin. If the spectral signature of seagrass and that of the background are sufficiently different and if data are available for a range of critical frequencies, it may be possible to distinguish between pixels that represent a mixed seagrass/background type and nearby pixels that represent the background alone. In practice however, sub-pixel spectral mixing remains the major limiting factor to the identification of land types (Hedley et al. 2012a; 2012b).

Importantly, while visual detection requires use of an RGB image (or a false-colour image using infrared as one of the three image bands), automated classification methods can be applied to multi-dimensional datasets such as multispectral and hyperspectral imagery, and usually perform better with this additional information (Islam et al. 2017).

## 4.3 Effects of water depth

Water depth is a critical factor influencing the detectability of benthic types. Overall, increased water depth reduces detectability due to the absorption of light by water molecules, but this absorption is much stronger for red light relative to blue light (Botha et al. 2013). This implies that if a benthic type can be detected because of a significantly different response in the blue (such as seagrass vs sand, see Figure 3), detectability of seagrass against sand can be achieved even at great depths (Kutser et al. 2020).

However, suspended sediment particles (turbidity) and other benthic types (e.g., reef, macroalgae beds or patches) tend to show similar spectral responses as seagrass in the blue region of the spectrum (Kutser et al. 2020). Multispectral sensors also tend to be designed to provide greater

spectral richness in the red region, making use of the fact that it is easier to differentiate vegetation types or characteristics in this part of the spectrum, which leaves few bands (two at most) in the blue part of the spectrum. As a result, the ability to detect seagrass decreases with water depth in cases other than in the ideal case above. Drones and aerial imagery of coastal benthic features are usually acquired at low tide to maximize detection capability in the intertidal zone. Satellite imagery should be selected, or tasked for acquisition, based on this criterion too.

## 4.4 Pricing of commercial imagery

The common pricing structure for commercial satellite imagery is on a per Area Of Interest (AOI) basis (polygon to be defined, with minimum area or dimensions possibly applying), at a rate per km² that depends on whether imagery is recent or not, and the number of bands and resolution required. For WorldView-2,3 imagery at full spatial resolution (<0.4 m) and spectral resolution (8 bands), the rates are (USD) $24/km² for imagery that is 90 days or older ("archive"), and $34/km² for more recent imagery ("fresh"). Minimum AOI size is 25 km² and minimum side-length is 2 km (for elongated AOIs, such as one following the coastline).

HBRC is interested in monitoring several areas around the coastline for seagrass, including an area of coastline approximately 6.5 km in length around Table Cape (Kahutara Point) on Māhia Peninsula, and a series of intertidal platforms and beaches between the northern edge of Kairakau Beach (approximately 39.935° S, 176.932° E) and the southern edge of the beach in Porangahau (approximately 40.315° S, 176.667° E), totalling approximately 54 km in length. According to the pricing structure above, this would constitute an order of two AOIs of 25 km² and 108 km², respectively (accounting for minimum area and width), that is a total order cost of approximately (USD) $3,200 for archive imagery or $4,500 for fresh imagery. Orders are typically put through a local reseller (in New Zealand, Critchlow Geospatial, Eagle Technology, and Xerra), who should be consulted to provide more accurate quotes at the time of ordering. Alternatively, one can subscribe to the Maxar Technologies online platform called SecureWatch, from which archive imagery can be accessed and downloaded with pricing based on usage. Pricing for the lowest SecureWatch tier is (USD) $5,000 per annum.

# 5 Conclusions

The detection and mapping of seagrass with multispectral satellite imagery is a mature field. Modern methods of classifying satellite imagery of a given optically-shallow area into its principal land/ seabed types (with one of them being seagrass) often yield high overall accuracy – in the 85-95% range (Moniruzzaman et al. 2019 Kutser et al. 2020). However, seagrass always occur as extensive meadows in these classification studies. Our review of the literature did not find studies attempting to detect very scarce patches of seagrass of small dimensions relative to the imagery spatial resolution.

The highest resolution available to date for satellite imagery is that of WorldView-2 and Worldview-3. Patches of seagrass of 2-3 m would occupy 7 to 10 pixels on its 0.31 m resolution panchromatic (greyscale) imagery and pansharpened RGB imagery, and 2 to 3 pixels on its eight 1.24 m resolution multispectral bands. These relative dimensions are at the edge of typical visual or automatic detection capabilities. The usefulness of the additional multispectral bands would also strongly depend on the type of background where seagrass patches occur, and the ability to differentiate between seagrass and other macrophytes or algae using spectral information. As a result, we cannot make a recommendation regarding the ability to detect seagrass patches in Hawke's Bay using satellite imagery without undertaking a small-scale trial. A detection experiment using sample WorldView-2,3 imagery over a ground-truthed area would be necessary to assess whether an efficient automated detection method can be devised and subsequently applied to larger scales.

Alternatively, other remote sensing technologies could be considered. In particular, the higher spatial and spectral resolutions of airborne hyperspectral imagery imply that these systems are more likely to be able to detect small seagrass patches. However, the complexity of these multidimensional datasets would require the use of automated detection approaches, rather than simple visual digitization.

In any case, we recommend that the field of remote sensing technology and the literature describing remote sensing for detection of seagrass should be closely monitored. There is currently a strong phase of technological development in platforms (e.g., drones battery life and range achievable, micro satellite constellations), sensors (e.g., lightweight hyperspectral imaging, synthetic aperture radar), and data mining/processing methods (e.g., machine learning approaches to computer vision), which may alter the content and conclusions of this assessment in the very near future. A perspective of the pace and capability of recent developments in spaceborne hyperspectral technology is provided by Giardino et al. (2019).

# 6 Acknowledgements

Becky Shanahan from Hawke's Bay Regional Council initiated this work and provided background information. Fleur Matheson and Sanjay Wadhwa (NIWA) were consulted, respectively, for their experience in seagrass ecology in Hawke's Bay and in remote sensing of intertidal habitats. This work was supported by the MBIE Envirolink Grant 2067-HBRC256, contract C01X1937.

# 7 Glossary of abbreviations and terms

| | |
|---|---|
| AOI | Area Of Interest |
| ASTER | Advanced Spaceborne Thermal Emission and Reflection Radiometer |
| CHRIS | Compact High Resolution Imaging Spectrometer |
| ESA | European Space Agency |
| ETM+ | Enhanced Thematic Mapper Plus |
| HBRC | Hawke's Bay Regional Council |
| HICO | Hyperspectral Imager for the Coastal Ocean |
| JAXA | Japan Aerospace Exploration Agency |
| MBIE | Ministry of Business, Innovation, and Employment |
| MODIS | Moderate Resolution Imaging Spectroradiometer |
| MSI | Multispectral Instrument |
| MSS | Multispectral Scanner System |
| NASA | National Aeronautics and Space Administration |
| NIR | Near infrared |
| NIWA | National Institute of Water and Atmospheric Research |
| OBIA | Object-Based Image Analysis |
| OLI | Operational Land Imager |
| PRISMA | Italian: PRecursore IperSpettrale della Missione Applicativa |
| RGB | Red, Green, Blue |
| SPOT | French: Satellite Pour l'Observation de la Terre |
| SWIR | Short-wave infrared |
| TIR | Thermal infrared |
| TIRS | Thermal Infrared Sensor |
| TM | Thematic Mapper |

# 8 References


Ackleson, S.G., Klemas, V. (1987) Remote sensing of submerged aquatic vegetation in lower Chesapeake Bay: A comparison of Landsat MSS to TM imagery. *Remote Sensing of Environment,* 22(2): 235–248.

Arias-Ortiz, A., Serrano, O., Masqué, P., Lavery, P.S., Mueller, U., Kendrick, G.A., Duarte, C.M., (2018) A marine heatwave drives massive losses from the world's largest seagrass: carbon stocks. *Nature Climate Change*, 8(4): 338–344.

Asner, G.P., Martin, R.E., Mascaro, J. (2017) Coral reef atoll assessment in the South China Sea using Planet Dove satellites. *Remote Sensing in Ecology and Conservation,* 3(2): 57–65.

Baumstark, R., Duffey, R., Pu, R. (2016) Mapping seagrass and colonized hard bottom in Springs Coast, Florida using WorldView-2 satellite imagery. *Estuarine, Coastal and Shelf Science,* 181: 83–92.

Bayyana, S., Pawar, S., Gole, S., Dudhat, S., Pande, A., Mitra, D., Sivakumar, K. (2020) Detection and mapping of seagrass meadows at Ritchie' s archipelago using Sentinel 2A satellite imagery. *Current Science*, 118(8): 1275–1282.

Botha, E.J., Brando, V.E., Anstee, J.M., Dekker, A.G., Sagar, S. (2013) Increased spectral resolution enhances coral detection under varying water conditions. *Remote Sensing of Environment,* 131: 247–261.

Casal, G., Kutser, T., Domínguez-Gómez, J.A., Sánchez-Carnero, N., Freire, J. (2011) Mapping benthic macroalgal communities in the coastal zone using CHRIS-PROBA mode 2 images. *Estuarine, Coastal and Shelf Science*, 94(3): 281–290. https://doi.org/10.1016/j.ecss.2011.07.008

Cerdeira-Estrada, S., Heege, T., Kolb, M., Ohlendorf, S., Uribe, A., Muller, A., Martell, R. (2012) Benthic habitat and bathymetry mapping of shallow waters in Puerto morelos reefs using remote sensing with a physics based data processing. In: *2012 IEEE International Geoscience and Remote Sensing Symposium*: 4383–4386. IEEE. https://doi.org/10.1109/IGARSS.2012.6350402

Cho, H.J., Ogashawara, I., Mishra, D., White, J., Kamerosky, A., Morris, L., Banisakher, D. (2014) Evaluating Hyperspectral Imager for the Coastal Ocean (HICO) data for seagrass mapping in Indian River Lagoon, FL. *GIScience & Remote Sensing*, 51(2): 120–138.

Duffy, J.P., Pratt, L., Anderson, K., Land, P.E., Shutler, J.D. (2018). Spatial assessment of intertidal seagrass meadows using optical imaging systems and a lightweight drone. *Estuarine, Coastal and Shelf Science*, 200: 169–180.

Fornes, A., Basterretxea, G., Orfila, A., Jordi, A., Alvarez, A., Tintore, J. (2006) Mapping Posidonia oceanica from IKONOS. *ISPRS Journal of Photogrammetry and Remote Sensing*, 60(5): 315–322.

Fourqurean, J.W., Duarte, C.M., Kennedy, H., Marbà, N., Holmer, M., Mateo, M.A., Serrano, O. (2012) Seagrass ecosystems as a globally significant carbon stock. *Nature Geoscience:* 5(7): 505–509.

Giardino, C., Brando, V.E., Gege, P., Pinnel, N., Hochberg, E., Knaeps, E., Dekker, A. (2019) Imaging Spectrometry of Inland and Coastal Waters: State of the Art, Achievements and Perspectives. *Surveys in Geophysics,* 40(3): 401–429.

Green, E.P., Short, F.T. (eds) (2003) *World Atlas of Seagrasses*. University of California Press, Berkeley, USA: 324.

Haggit, T., Wade, O. (2016) Hawke's Bay Marine Information: Review and Research Strategy. *eCoast Client Report*. Prepared for Hawkes Bay Regional Council: 113.

Hedley, J.D., Roelfsema, C.M., Phinn, S.R., Mumby, P.J. (2012b) Environmental and Sensor Limitations in Optical Remote Sensing of Coral Reefs: Implications for Monitoring and Sensor Design. *Remote Sensing,* 4(1): 271–302.

Hedley, J., Roelfsema, C., Chollett, I., Harborne, A., Heron, S., Weeks, S., Mumby, P. (2016) Remote Sensing of Coral Reefs for Monitoring and Management: A Review. *Remote Sensing,* 8(2): 118.

Hedley, J., Roelfsema, C., Koetz, B., Phinn, S. (2012a) Capability of the Sentinel 2 mission for tropical coral reef mapping and coral bleaching detection. *Remote Sensing of Environment,* 120: 145–155.

Hemminga, M., Duarte, C. (2000) *Seagrass Ecology*. Cambridge: Cambridge University Press.

Hossain, M.S., Bujang, J.S., Zakaria, M.H., Hashim, M. (2014) The application of remote sensing to seagrass ecosystems: an overview and future research prospects. *International Journal of Remote Sensing*, 36(1).

Inglis, G.J. (2003) The seagrasses of New Zealand. In: Green, E.P., Short, F.T. (eds): *World atlas of seagrasses.* University of California Press, Berkeley: 148–157.

Islam, S.M.S., Raza, S.K., Moniruzzamn, M., Janjua, N., Lavery, P., Al-Jumaily, A. (2017) Automatic seagrass detection: A survey, *2017 International Conference on Electrical and Computing Technologies and Applications (ICECTA):* 1–5.

Israel, S.A., Fyfe, J.E. (1996) Determining the sensitivity of SPOT XS imagery for monitoring intertidal and sublittoral vegetation of Otago Harbour. *Conservation Advisory Science Notes*, No. 131. Department of Conservation, Wellington.

Knudby, A., Nordlund, L. (2011) Remote sensing of seagrasses in a patchy multi-species environment. *International Journal of Remote Sensing*, 32(8): 2227–2244.

Knudby, A., Newman, C., Shaghude, Y., Muhando, C. (2010) Simple and effective monitoring of historic changes in nearshore environments using the free archive of Landsat imagery. *International Journal of Applied Earth Observation and Geoinformation,* 12(SUPPL. 1): S116–S122.

Kovacs, E., Roelfsema, C., Lyons, M., Zhao, S., Phinn, S. (2018) Seagrass habitat mapping: how do Landsat 8 OLI, Sentinel-2, ZY-3A, and Worldview-3 perform? *Remote Sensing Letters,* 9(7): 686–695.

Kutser, T., Hedley, J., Giardino, C., Roelfsema, C., Brando, V.E. (2020) Remote sensing of shallow waters – A 50 year retrospective and future directions. *Remote Sensing of Environment*, 240: 111619.

Luczkovich, J., Wagner, T., Michalek, J., Stoffle, R. (1993) Discrimination of coral reefs, seagrass meadows, and sand bottom types from space: a Dominican Republic case study. *Photogrammetric Engineering and Remote Sensing*, 59(3): 385–389.

Lundquist, C.J., Jones, T.C., Parkes, S.M., Bulmer, R.H. (2018) Changes in benthic community structure and sediment characteristics after natural recolonisation of the seagrass *Zostera muelleri*. *Scientific Reports*, 8(1): 13250.

Lyons, M.B., Phinn, S.R., Roelfsema, C.M. (2012) Long term land cover and seagrass mapping using Landsat and object-based image analysis from 1972 to 2010 in the coastal environment of South East Queensland, Australia. *ISPRS Journal of Photogrammetry and Remote Sensing*, 71: 34–46.

Lyons, M.B., Roelfsema, C.M., Phinn, S.R. (2013) Towards understanding temporal and spatial dynamics of seagrass landscapes using time-series remote sensing. *Estuarine, Coastal and Shelf Science,* 120: 42–53.

Lyons, M., Phinn, S., Roelfsema, C. (2011) Integrating Quickbird Multi-Spectral Satellite and Field Data: Mapping Bathymetry, Seagrass Cover, Seagrass Species and Change in Moreton Bay, Australia in 2004 and 2007. *Remote Sensing,* 3(1): 42–64.

Madarasz-Smith, A., Shanahan, B. (2020) State of the Hawke's Bay Coastal Marine Environment: 2013 to 2018. *Hawkes Bay Regional Council Publication,* No. 5425: 136.

Manuputty, A., Lumban Gaol, J., Agus, S.B. (2015) Seagrass Mapping Based on Satellite Image Worldview-2 by Using Depth Invariant Index Method. *ILMU KELAUTAN: Indonesian Journal of Marine Sciences*: 21(1), 37.

Marcello, J., Eugenio, F., Marques, F., Martin, J. (2015) Precise classification of coastal benthic habitats using high resolution Worldview-2 imagery. In: *2015 IEEE International Geoscience and Remote Sensing Symposium (IGARSS*), Vol. 2015-Novem: 2307–2310.

Matheson, F. (2018) Seagrass assessment for Pōrangahau Estuary, Hawkes Bay. *NIWA client report* 2018301HN. Prepared for Hawkes Bay Regional Council: 19

Matheson, F.E., Lundquist, C.J., Gemmill, C.E.C., Pilditch, C.A. (2011) New Zealand seagrass – more threatened than IUCN review indicates. *Biological Conservation,* 144: 2749-2750.

Mishra, D., Narumalani, S., Rundquist, D., Lawson, M. (2006) Benthic Habitat Mapping in Tropical Marine Environments Using QuickBird Multispectral Data. *Photogrammetric Engineering & Remote Sensing*, 72(9): 1037–1048.

Moniruzzaman, M., Islam, S.M.S., Lavery, P., Bennamoun, M., Lam, C.P. (2019) *Imaging and Classification Techniques for Seagrass Mapping and Monitoring: A Comprehensive Survey.* arxiv.org/abs/1902.11114

Mumby, P.J., Edwards, A.J. (2002). Mapping marine environments with IKONOS imagery: enhanced spatial resolution can deliver greater thematic accuracy. *Remote Sensing of Environment,* 82(2–3): 248–257.

Mumby, P., Green, E., Edwards, A., Clark, C. (1997) Measurement of seagrass standing crop using satellite and digital airborne remote sensing. *Marine Ecology Progress Series*, 159: 51–60.

Park, S. (2016) Extent of seagrass in the Bay of Plenty in 2011. Environmental Publication 2016/03. Bay of Plenty Regional Council, Whakatane, New Zealand. Available at https://cdn.boprc.govt.nz/media/509090/extent-of-seagrass-in-the-bay-of-plenty-in-2011.pdf

Park, S.G. (1999) Changes in abundance of seagrass (*Zostera* spp.) in Tauranga Harbour from 1959–1996. *Environmental Report,* 99/30. Environment Bay of Plenty, Whakatane: 19.

Petus, C., Collier, C., Devlin, M., Rasheed, M., McKenna, S. (2014) Using MODIS data for understanding changes in seagrass meadow health: A case study in the Great Barrier Reef (Australia). *Marine Environmental Research,* 98: 68–85.

Pham, T.D., Xia, J., Ha, N.T., Bui, D.T., Le, N.N., Tekeuchi, W. (2019) A Review of Remote Sensing Approaches for Monitoring Blue Carbon Ecosystems: Mangroves, Seagrasses and Salt Marshes during 2010–2018. *Sensors,* 19(8): 1933.

Phinn, S., Roelfsema, C., Dekker, A., Brando, V., Anstee, J. (2008) Mapping seagrass species, cover and biomass in shallow waters: An assessment of satellite multi-spectral and airborne hyper-spectral imaging systems in Moreton Bay (Australia). *Remote Sensing of Environment,* 112(8): 3413–3425.

Pu, R., Bell, S. (2013) A protocol for improving mapping and assessing of seagrass abundance along the West Central Coast of Florida using Landsat TM and EO-1 ALI/Hyperion images. *ISPRS Journal of Photogrammetry and Remote Sensing,* 83: 116–129.

Pu, R., Bell, S. (2017) Mapping seagrass coverage and spatial patterns with high spatial resolution IKONOS imagery. *International Journal of Applied Earth Observation and Geoinformation*, 54: 145–158.

Pu, R., Bell, S., Meyer, C., Baggett, L., Zhao, Y. (2012) Mapping and assessing seagrass along the western coast of Florida using Landsat TM and EO-1 ALI/Hyperion imagery. *Estuarine, Coastal and Shelf Science*, 115(March 2018): 234–245.

Robertson, B., Gillespie, P., Asher, R., Frisk, S., Keeley, N., Hopkins, G., Tuckey, B. (2002) Estuarine Environmental Assessment and Monitoring: A National Protocol. *Part A - Development of the Monitoring Protocol for New Zealand Estuaries: introduction,*

*rationale and methodology*. Prepared for Supporting Councils and the Ministry for the Environment, Sustainable Management Fund, Contract No. 5096.

Roelfsema, C.M., Lyons, M., Kovacs, E.M., Maxwell, P., Saunders, M.I., Samper-Villarreal, J., Phinn, S.R. (2014) Multi-temporal mapping of seagrass cover, species and biomass: A semi-automated object based image analysis approach. *Remote Sensing of Environment*, 150: 172–187.

Roelfsema, C., Kovacs, E.M., Saunders, M.I., Phinn, S., Lyons, M., Maxwell, P. (2013) Challenges of remote sensing for quantifying changes in large complex seagrass environments. *Estuarine, Coastal and Shelf Science*, 133: 161–171.

Shapiro, A.C., Rohmann, S.O. (2006) Mapping changes in submerged aquatic vegetation using Landsat imagery and benthic habitat data: Coral reef ecosystem monitoring in Vieques Sound between 1985 and 2000. *Bulletin of Marine Science*, 79(2): 375–388.

Su, L., Huang, Y. (2019) Seagrass Resource Assessment Using WorldView-2 Imagery in the Redfish Bay, Texas. *Journal of Marine Science and Engineering*, *7*(4), 98.

Torres-Madronero, M.C., Velez-Reyes, M., Goodman, J.A. (2014) Subsurface unmixing for benthic habitat mapping using hyperspectral imagery and lidar-derived bathymetry. In: M. Velez-Reyes & F. A. Kruse (Eds*). Algorithms and Technologies for Multispectral, Hyperspectral, and Ultraspectral Imagery XX*, Vol. 9088: 90880M.

Traganos, D., Reinartz, P. (2018) Machine learning-based retrieval of benthic reflectance and Posidonia oceanica seagrass extent using a semi-analytical inversion of Sentinel-2 satellite data. *International Journal of Remote Sensing*, 39(24): 9428–9452.

Traganos, D., Aggarwal, B., Poursanidis, D., Topouzelis, K., Chrysoulakis, N., Reinartz, P. (2018) Towards global-scale seagrass mapping and monitoring using Sentinel-2 on Google Earth Engine: The case study of the Aegean and Ionian Seas. *Remote Sensing*, 10(8): 1–14.

Turner, S., Schwarz, A.M. (2006) Management and conservation of seagrass in New Zealand: an introduction. *Science for Conservation,* 264: 90.

Uhrin, A.V., Townsend, P.A. (2016) Improved seagrass mapping using linear spectral unmixing of aerial photographs. *Estuarine, Coastal and Shelf Science,* 171: 11–22.

Urbański, J., Mazur, A., Janas, U. (2009) Object-oriented classification of QuickBird data for mapping seagrass spatial structure. *Oceanological and Hydrobiological Studies*, 38(1): 27–43.

Vahtmäe, E., Kutser, T., Kotta, J., Pärnoja, M., Möller, T., Lennuk, L. (2012) Mapping Baltic Sea shallow water environments with airborne remote sensing. *Oceanology,* 52(6): 803–809.

Valle, M., Palà, V., Lafon, V., Dehouck, A., Garmendia, J.M., Borja, Á., Chust, G. (2015) Mapping estuarine habitats using airborne hyperspectral imagery, with special focus on seagrass meadows. *Estuarine, Coastal and Shelf Science*, 164: 433–442.

Wang, C.K., Philpot, W.D. (2007) Using airborne bathymetric lidar to detect bottom type variation in shallow waters. *Remote Sensing of Environment*, 106(1): 123–135.

Waycott, M., Duarte, C.M., Carruthers, T.J.B., Orth, R.J., Dennison, W.C., Olyarnik, S., Williams, S.L. (2009) Accelerating loss of seagrasses across the globe threatens coastal ecosystems. *Proceedings of the National Academy of Sciences,* 106(30): 12377–12381.

# Appendix A Additional information on spaceborne multispectral and hyperspectral sensors

**Table A.1: Detail on spaceborne multispectral and hyperspectral sensors mentioned in this report**

| Sensor | Type | Carrier satellite | Operator | Scientific / Commercial | Spatial resolution at nadir (m) | Bands | Dates |
|---|---|---|---|---|---|---|---|
| Hyperion | HS | Earth Observing-1 | NASA | Scientific | HS: 30 | HS: 220 | 2001-2015 |
| CHRIS | HS | PROBA-1 | | | HS: 18 | | 2001- |
| HICO | HS | International Space Station | | Scientific | HS: 90 | | 2009-2014 |
| PRISMA | HS | PRISMA | | | HS: 30 | | 2019- |
| Advanced Land Imager (ALI) | MS | Earth Observing-1 | NASA | Scientific | Pan: 10<br>MS: 30 | MS: 10 | 2000-2017 |
| Operational Land Imager (OLI) | MS | Landsat 8 | NASA/USGS | Scientific | Pan: 15<br>MS/SWIR: 30 | MS: 6 (Coastal, B, G, R, NIR, Cirrus)<br>SWIR: 2 | 2013- |
| Landsat Enhanced Thematic Mapper Plus (ETM+) | MS | Landsat 7 | NASA/USGS | Scientific | Pan: 15<br>MS/SWIR: 30 | MS: 4 (B, G, R, NIR)<br>SWIR: 2 | 1999- |
| Landsat Thematic Mapper (TM) | MS | Landsat 4, 5 | NASA/USGS | | MS: 30 | | |
| Landsat Multispectral Scanner (MSS) | MS | Landsat 1, 2, 3, 4, 5 | NASA/USGS | | 60 | | 1972-1992 |
| MSI | MS | Sentinel-2 | ESA | Scientific | Multiple: 10, 20, 60 | MS: 10 (Coastal, B, G, R, Red edge 1/2/3, NIR, Water vapour<br>SWIR: 3 | 2015- |

| Sensor | Type | Carrier satellite | Operator | Scientific / Commercial | Spatial resolution at nadir (m) | Bands | Dates |
|---|---|---|---|---|---|---|---|
| SpaceView 110 | MS | WorldView-4 (formerly GeoEye-2) | MAXAR (formerly DigitalGlobe) | Commercial | Pan: 0.31<br>MS: 1.24 | MS: 4 (B, G, R, NIR) | 2016-2019 |
| WV110 | MS | WorldView-3 | MAXAR (formerly DigitalGlobe) | Commercial | Pan: 0.31<br>MS: 1.24<br>SWIR: 3.7<br>CAVIS: 30 | MS: 8 (R, R edge, Coastal, B, G, Y, NIR, NIR-2)<br>SWIR: 8<br>CAVIS: 12 | 2014- |
| WV110 | MS | WorldView-2 | MAXAR (formerly DigitalGlobe) | Commercial | Pan: 0.46<br>MS: 1.85 | MS: 8 (R, R edge, Coastal, B, G, Y, NIR, NIR-2) | 2009- |
| | Pan | WorldView-1 | MAXAR (formerly DigitalGlobe) | Commercial | Pan: 0.5 | N/A | 2007- |
| | MS | GeoEye-1 | MAXAR (formerly DigitalGlobe) | Commercial | Pan: 0.41<br>MS: 1.64 | MS: 4 (B, G, R, NIR) | 2008- |
| BGIS 2000 | MS | QuickBird-2 | MAXAR (formerly DigitalGlobe) | Commercial | Pan: 0.60<br>MS: 2.40 | MS: 4 (B, G, R, NIR) | 2001-2014 |
| OSA | MS | IKONOS | MAXAR (formerly DigitalGlobe) | Commercial | Pan: 0.82<br>MS: 3.28 | MS: 4 (B, G, R, NIR) | 2000-2015 |
| | MS | Pleiades (1A and 1B) | Airbus | Commercial | Pan: 0.5<br>MS: 2.0 | MS: 4 (B, G, R, NIR) | 2011- |
| | MS | SPOT 6/7 | Airbus | Commercial | Pan: 1.5<br>MS: 6.0 | MS: 4 (B, G, R, NIR) | 2012- |
| SPOT High Resolution Visible (HRV) multi-spectral mode (XS) | MS | SPOT 1, 2, 3 | | | Pan: 10<br>MS: 20 | MS: 3 (G, R, NIR) | 1986-2009 |

| Sensor | Type | Carrier satellite | Operator | Scientific / Commercial | Spatial resolution at nadir (m) | Bands | Dates |
|---|---|---|---|---|---|---|---|
| HRVIR | MS | SPOT 4 | | | Pan: 10 | | 1998-2013 |
| high resolution geometrical (HRG) | MS | SPOT 5 | | | Pan: 2.5<br>MS: 10 | | 2002- |
| | MS | SkySat (constellation) | Planet Labs | Commercial | Pan: 0.5 (formerly 0.8)<br>MS: 1.0 | MS: 4 (B, G, R, NIR) | 2014- |
| | | PlanetScope (constellation) | Planet Labs (US) | Commercial | Pan: 1.5<br>MS: 3-5 | MS: 4 (B, G, R, NIR) | |
| | MS | Ziyuan-3A | MLR (China) | | 2.5<br>Infrared: 6 | | 2012- |
| | MS | SuperView-1 | | | Pa: 0.5<br>MS: 2.0 | MS: 4 (B, G, R, NIR) | 2018- |